Contents lists available at ScienceDirect

Arthroplasty Today

Original Research

Magnetic Resonance Safety Evaluation of a Novel Alumina Matrix Composite Ceramic Knee and Image Artifact Comparison to a Metal Knee Implant of Analogous Design

Yvonne Mödinger, PhD [a, *], Eric D. Anttila, PhD [b], Grant M. Baker, MS [b],
David C. Gross, PhD [b], Alessandro A. Porporati, PhD [a, c]

[a] Medical Products Division, CeramTec GmbH, Plochingen, Germany
[b] MED Institute Inc., West Lafayette, IN, USA
[c] Department of Engineering and Architecture, University of Trieste, Trieste, Italy

ABSTRACT

Background: Image artifacts caused by metal knee implants in 1.5T and 3T magnetic resonance imaging (MRI) systems complicate imaging-based diagnosis of the peri-implant region after total knee arthroplasty. Alternatively, metal-free knee prostheses could effectively minimize MRI safety hazards and offer the potential for higher quality diagnostic images.

Methods: A novel knee arthroplasty device composed of BIOLOX delta, an alumina matrix composite (AMC) ceramic, was tested in a magnetic resonance (MR) environment. American Society for Testing and Materials test methods were used for evaluating magnetically induced displacement force, magnetically induced torque, radiofrequency-induced heating, and MR image artifact.

Results: Magnetically induced displacement force and magnetically induced torque results of the AMC ceramic knee indicated that these effects do not pose a known risk in a clinical MR environment, as assessed in a 3T magnetic field. Moreover, minimal radiofrequency-induced heating of the device was observed. In addition, the AMC ceramic knee demonstrated minimal MR image artifacts (7 mm) in comparison to a cobalt-chromium knee (88 mm). The extremely low magnetic susceptibility of AMC (2 ppm) underlines that it is a nonmetallic and nonmagnetic material well suited for the manufacturing of MR Safe orthopaedic implants.

Conclusions: The AMC ceramic knee is a novel metal-free total knee arthroplasty device that can be regarded as MR Safe, as suggested by the absence of hazards from the exposure of this implant to a MR environment. The AMC ceramic knee presents the advantage of being scanned with superior imaging results in 3T MRI systems compared to alternative metal implants on the market.

Introduction

Ceramics have been used as orthopaedic implant materials for total joint arthroplasty for decades. Alumina-based ceramics, in particular, have an excellent track record of biocompatibility and high wear resistance [1–7]. However, unlike the widespread use of ceramics in hip arthroplasty, most knee prostheses are composed of metal femoral (mainly cobalt-chromium [CoCr]) and tibial (mainly titanium [Ti] or CoCr) components combined with a polyethylene (PE) insert. Ceramic implant alternatives in total knee arthroplasty (TKA) have yet to gain acceptance among orthopaedic surgeons [8]. There is clinical need for nonmetallic knee implants due to metal corrosion-induced ion release at the implant site and high abundance of wear-induced PE particles with metal compared to ceramic as tribological pairing [9–15]. Both metal ions and wear debris are suspected causes of implant-associated pathology and subsequent implant failure [11,16,17]. Adverse local tissue reaction (ALTR) around the implant arises from inflammatory responses to wear particles and is regarded as an origin of pain, instability, and arthroplasty dysfunction [18]. Moreover, metal wear and metal ions

* Corresponding author. CeramTec-Platz 1-9, Plochingen 73207, Germany. Tel.: +49 160 3855716.
E-mail address: y.moedinger@ceramtec.de

are suspected to facilitate periprosthetic joint infection (PJI) [19,20]. In case of both ALTR and PJI, high-quality imaging of the affected implant site can be helpful for postoperative medical treatment. Studies have described a reduced risk for PJI with ceramic compared to metal bearings in hip arthroplasty [20–25].

Implant failure due to metal allergy, a type IV delayed hypersensitivity reaction to ions released from the implanted metallic device, is another clinical complication where ceramic implants can provide an alternative for patients with signs of allergic reactions [26,27]. Diagnosis of metal hypersensitivity is, however, challenging, and diagnostic tests for metal allergens are not always conclusive or do not fully reflect the periprosthetic tissue response [28,29]. Although the lymphocyte transformation test (LTT) is thought to be more sensitive than the patch test on skin, LTT is not readily available, and blood testing comes at higher material and time expenses [30]. Of note, it was shown recently that there is little relationship between positive LTT results and the synovial tissue response to TKA implants and revision outcomes [31,32].

Knee implant longevity is becoming increasingly important, given the dramatically increased numbers of primary and revision TKA surgeries in ever-younger patients (65 and younger) [33–36], who are mostly active and knee-loading. Material safety of the implant in the magnetic resonance imaging (MRI) environment is another need arising from clinical practice [37]. An estimated 1.18 million people underwent knee arthroplasty surgery in the United States in 2021 [38] with projections of exceeding 1.9 million TKA surgeries in 2030 [39]. Albeit routine, postoperative care involves conventional radiographic imaging; many patients undergo MRI, for example, to evaluate reasons for stiffness or nonspecific knee pain, which are common complications after TKA [40]. Also, patients with suspected periprosthetic pathology, such as damage of the surrounding soft tissues, ALTR, osteolysis, implant loosening, or infections might not routinely undergo MRI [41–47]. In comparison with other imaging modalities, MRI can offer additional soft tissue diagnosis, and compared to computed tomography, in particular, MRI provides superior soft tissue contrast, easier assessment of periprosthetic anatomical structures while not exposing the patient to ionizing radiation [46,48].

When metallic implants are introduced into the strong external magnetic field of MRI systems, which are commonly 1.5 Tesla (T) or 3T in clinical practice, these devices can become potential safety hazards for patients by displacement due to the magnetic field or heating due to radiofrequency pulses, also of the adjacent tissue [45,49]. Metal implants that have been demonstrated to pose no known hazards in a magnetic resonance (MR) environment with specified conditions of use are referred to as "MR Conditional," thus allowing the patient to be scanned only if additional conditions for safe use are met. Moreover, material magnetization of metallic implants is influencing the MR image artifact at the bone/prosthesis interface [45,50]. Thus, MR technologists and radiologists face potential problems with image distortion and misregistration of the acquired image signal possibly resulting in uninterpretable or nondiagnostic images or images mimicking nonexisting disease [51,52]. To overcome this problem, MRI scanning sequences were optimized, and advanced techniques have been developed, such as multiacquisition variable-resonance image combination, metal artifact reduction sequence, or slice encoding for metal artifact correction [50,53], with slice encoding for metal artifact correction being largely applied in knee implant imaging [52,54]. However, even with improved scanning modes, it remains challenging to detect reasonable MRI abnormalities of metal implants in arthroplasty to support clinical decision-making [46,50,55].

The purpose of this study was to evaluate a novel ceramic TKA device without metallic components (ie, metal-free) to determine any device hazards resulting from a clinically relevant MR environment. Standardized test methods were applied to investigate magnetically induced displacement force, magnetically induced torque, and radiofrequency (RF)-induced heating of the implant. In addition, the extent of MR image artifacts was evaluated, and results were compared to a metal (CoCr) knee implant of analogous design. The magnetic susceptibility of alumina matrix composite (AMC) ceramic and metal alloys (CoCr and Ti) was assessed to further describe material interactions with and distortion of the applied magnetic field.

Material and methods

Test materials

A total knee replacement implant (CeramTec GmbH, Plochingen, Germany) consisting of a femoral and tibial component made with AMC (BIOLOX *delta*, CeramTec GmbH, Plochingen, Germany) and a vitamin E cross-linked insert was tested to evaluate magnetically induced displacement force, magnetically induced torque, RF-induced heating, and MR image artifacts.

An analogous CoCr knee implant consisting of a femoral and tibial CoCr component and an ultra-high molecular weight PE insert was tested to evaluate MR image artifacts.

Cylindrical shaped BIOLOX *delta* ceramic, CoCr alloys, and Ti alloys (diameter of 3.2 mm, length of approx. 4 cm) were used for magnetic susceptibility testing.

BIOLOX *delta* is a ceramic composite consisting of yttria-stabilized zirconia grains (17 vol%) and platelet-shaped crystals of strontium hexa-aluminate (3 vol%) that are homogenously dispersed in the fine-grained alumina matrix (80 vol%).

MRI systems used for testing

A 3T MAGNETOM Prisma MRI scanner (Siemens Healthcare GmbH, Erlangen, Germany) operating at resonance frequency of 123 MHz was used for assessment of MR image artifacts. A 3T Discovery MR750 MRI scanner (GE Healthcare, Chicago, IL) operating at resonance frequency of 128 MHz was used for evaluating magnetically induced displacement force, magnetically induced torque, and RF-induced heating.

Magnetically induced displacement force

Magnetically induced displacement force was evaluated in a 3T MRI system using the deflection angle test method outlined in American Society for Testing and Materials (ASTM) Standard Test Method F2052-21 [56]. The implant was mounted onto a custom fixture at a location of known static magnetic field strength and magnetic spatial gradient. The resulting deflection angle (α) was used to calculate the magnetically induced displacement force.

Magnetically induced torque

Magnetically induced torque was evaluated according to ASTM F2213-17 [57] using the equation displayed in the Supplement. The test article was placed on a low-friction acrylic surface centered near the isocenter of the scanner. The test article was subsequently rotated in 45° increments and observed for movement.

Radiofrequency (RF)-induced heating

RF-induced heating was evaluated according to ASTM F2182-19e2 [58]. The temperature rise of the implant was measured in a gelled saline phantom (1.32 g/L NaCl and 10 g/L polyacrylic acid in distilled water). The electrical conductivity of the gelled saline was

Table 1
Measured and scaled maximum temperature rise for the AMC ceramic knee in a 3T MRI system after 15 minutes of RF-induced heating.

Description	Scan time (min)	Whole phantom average SAR (W/kg)	Maximum temperature rise (°C)			
			Probe 1	Probe 2	Probe 3	Probe 4
AMC ceramic knee	15	1.3	0.66	0.86	0.75	0.21
		4.0[a]	1.64	2.14	1.87	0.52
Background (no test article)		1.3	0.48	0.31	0.58	0.19

SAR, specific absorption rate.
  [a] The maximum temperature values are scaled from 1.3 W/kg to 4.0 W/kg.

0.47 ± 10% S/m at room temperature (22°C). The Luxtron Fiber Optic Thermometry Probe STF-5M (Advanced Energy, Denver, CO, US) recorded temperatures with a resolution of 0.01°C and temporal resolution of 1 s. Positioning of the fiber optic thermometry probes (Fig. S2), details on MRI acquisition parameters (Table S1), and calculation of temperature rise are provided as Supplement.

Magnetic resonance image artifact

MR image artifact of the AMC ceramic knee and the CoCr knee was assessed according to ASTM F2119-07 (2013) [59]. The implants were immersed in a copper sulfate solution (2 g/L). Spin echo and gradient echo pulse sequences were used to acquire image pairs with and without (background) the implants in each orientation (axial, coronal, and sagittal). The distance from the test article boundary to the fringe of artifact (±30% zone) was measured. Digital Imaging and Communications in Medicine image with the implant was subtracted from the background and filtered to show only the pixels that changed by >30% according to a custom MATLAB code. For each image, the approximate dimension of the implant was removed from the artifact measurement and divided in half, providing the image artifact distance. MRI system scanning parameters are provided as Supplement (Table S2).

For performance of the described tests, the United States Food and Drug Administration guidance document *Testing and Labeling Medical Devices for Safety in the Magnetic Resonance (MR) Environment* [60] was followed in addition to the relevant ASTM standards.

Magnetic susceptibility

Volumetric magnetic susceptibility of AMC ceramic, CoCr alloys and Ti alloys was calculated using an MSB Mk1 Evans Balance (Sherwood Scientific Ltd., Cambridge, UK) and then converted to units of parts per million (ppm).

No institutional review board approval was required for this in vitro study.

Results

Magnetically induced displacement force

The maximum deflection angle measured for the AMC ceramic knee at the test location ($\alpha_l = 0°$) and the deflection angle calculated at the desired labeling MRI safety conditions ($\alpha_c = 0°$) demonstrated that no magnetically induced displacement force ($F_m = 0$ N) acted on the device; therefore, the force due to gravity (F_g) of 4.2 N is greater than any other force present on the implant in the MR environment.

Magnetically induced torque

The AMC ceramic knee remained static during the test, and therefore, the magnetically induced torque of the device (τ_{mag}) was less than the cross product of the friction force between the test article and acrylic table and the test article length (0.18 N m). For comparison, torque due to the earth's gravity (τ_{grav}) of the device was 0.59 N m.

RF-induced heating

Results for RF-induced heating are shown in Table 1 and Figure 1. The AMC ceramic knee demonstrated minimal temperature rise (less than 1°C) after 15 minutes of scan time in a 3T MRI system with a whole phantom averaged specific absorption rate of 1.3 W/kg. After scaling the whole phantom's averaged specific absorption rate to 4.0 W/kg to simulate first level operating mode, the temperature rise was approximately 2.1°C.

Magnetic resonance image artifact

Results for MR image artifact distance within a 3T MRI system for both implants are shown in Table 2. The maximum image artifact distances were 6 mm and 7 mm for the AMC ceramic knee and 69 mm and 88 mm for the CoCr knee using a spin echo and gradient echo pulse sequence, respectively.
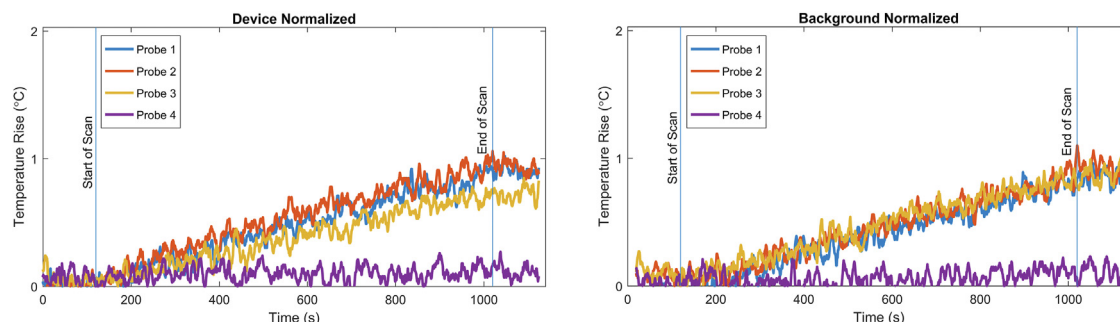

Figure 1. RF-induced temperature rises for the AMC ceramic knee after 15 minutes of scanning in a 3T MRI system, normalized to the initial temperature.

Table 2
Maximum image artifact distance for each scan orientation with SE and GRE pulse sequences for the AMC ceramic knee and the CoCr knee.

Description	Sequence	Orientation	Artifact dimension (mm)	Test article dimension (mm)	Artifact distance (mm)
AMC ceramic knee	SE	Axial	84	81	2
		Coronal	92	81	6
		Sagittal	144	140	2
	GRE	Axial	95	81	7
		Coronal	94	81	6
		Sagittal	154	140	7
CoCr knee	SE	Axial	155	75	40
		Coronal	213	75	69
		Sagittal	259	140	60
	GRE	Axial	252	75	88
		Coronal	269	140	64
		Sagittal	305	140	82

SE, spin echo; GRE, gradient echo.

Images of the implant, respective background images, and resulting MR image artifacts are shown for the AMC ceramic knee (Figs. 2 and 3) and CoCr knee (Figs. 4 and 5).

All results of the hazard tests and the assessment of MR image artifacts are summarized in Table 3, according to recommendations and relevant guidelines [60,61].
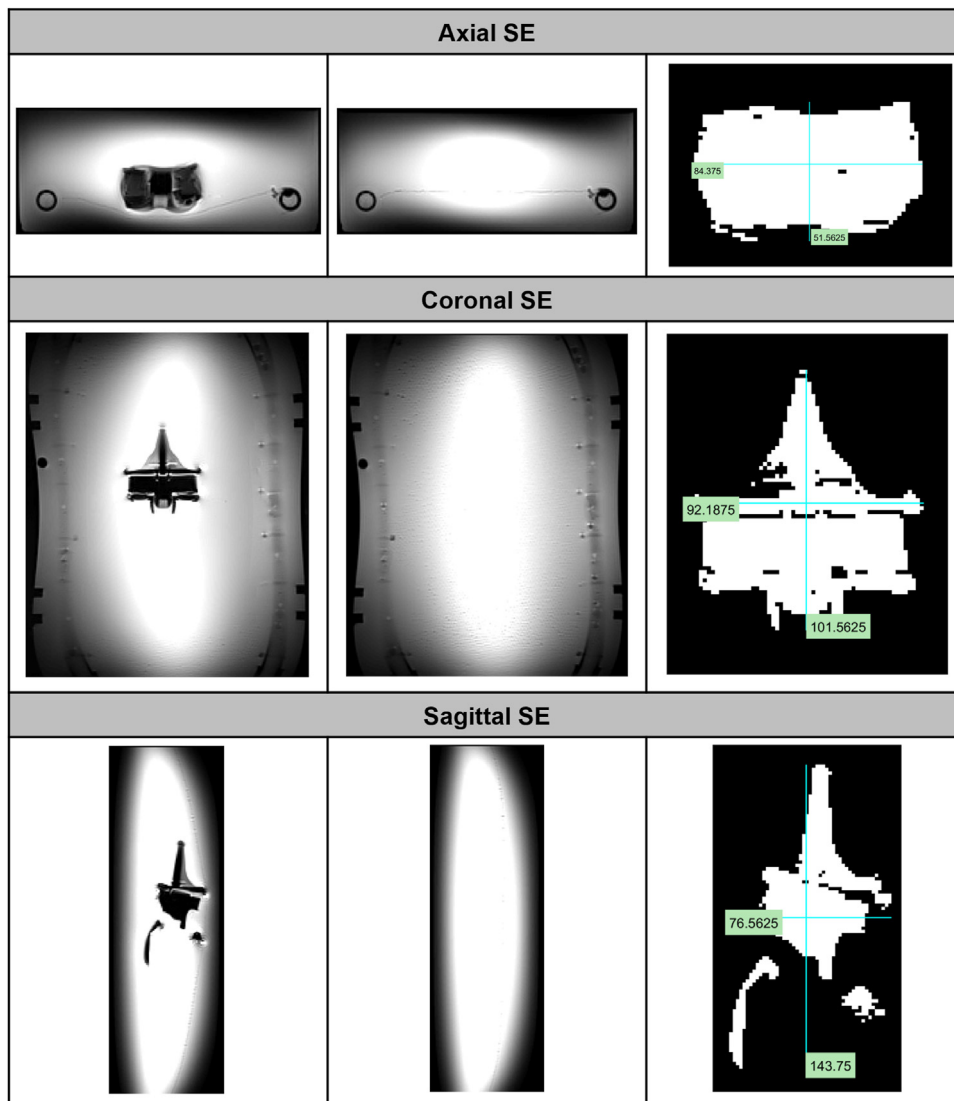

Figure 2. AMC ceramic knee with a spin echo pulse sequence in a 3T MRI system. Worst-case image (left), background image (middle), resulting image artifact (right). Measurements are in millimeters.

Figure 3. AMC ceramic knee with a gradient echo pulse sequence in a 3T MRI system. Worst-case image (left), background image (middle), resulting image artifact (right). Measurements are in millimeters.
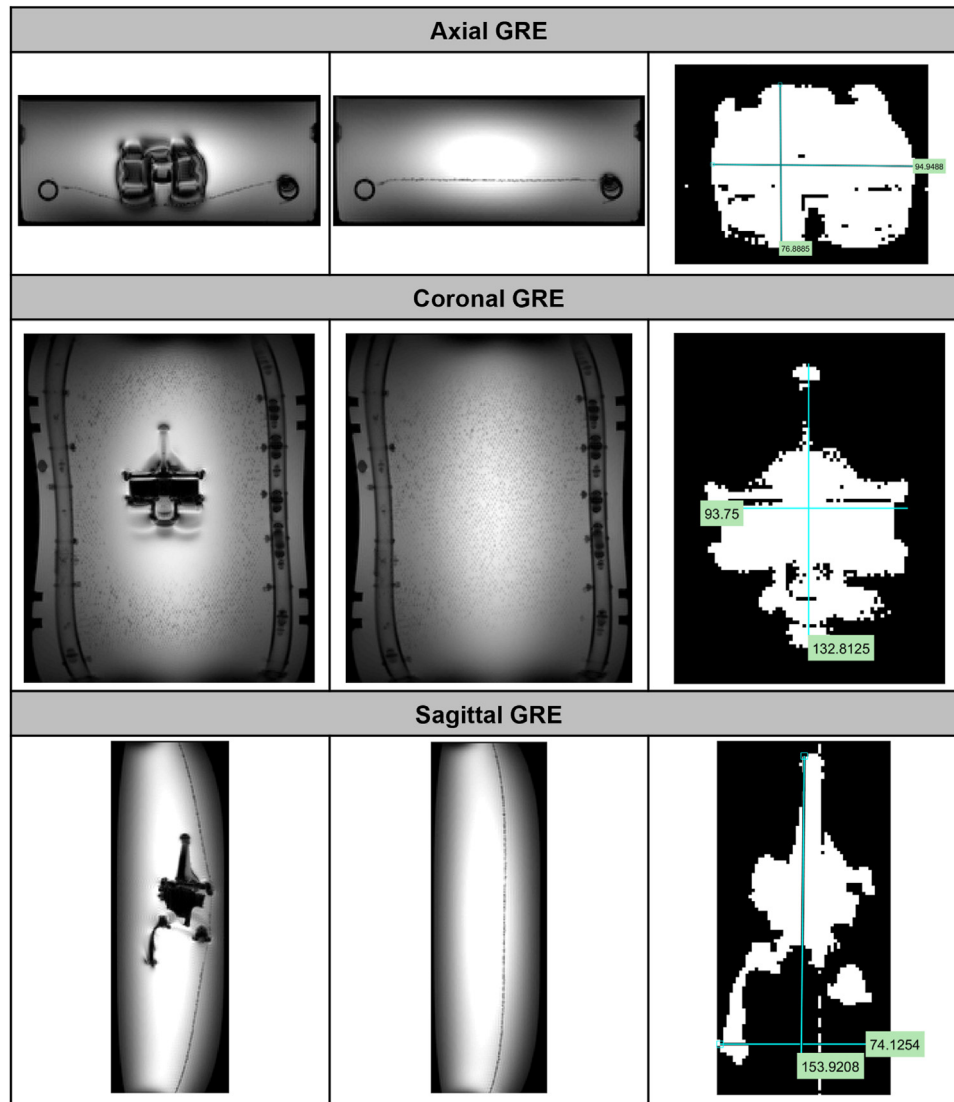
Magnetic susceptibility

The magnetic susceptibility of the AMC ceramic and of medical-grade metal alloys (CoCr and Ti) commonly used in orthopaedic applications were determined (Table 4).

Discussion

Primary and revision knee arthroplasty is increasing due to an aging population and rising TKA procedures also in younger patients [33,35,62]. Due to this increase, postoperational MRI-based evaluations of the knee implant area are gaining importance. Moreover, a number of patients (10-20%) remain unsatisfied after TKA procedures [63–65], for instance due to pain at rest or limited range of motion [66], and MRI might aid in diagnostics of these cases. Technical advances in MRI allow postarthroplasty diagnoses of the knee joint and adjacent tissues in cases of suspected pathology. However, the device material impacts image quality and, in consequence, influence quality of diagnosis and clinical decision-making. Metal alloys are commonly used as knee implants,

which, based on the nature of the material, interact with and distort the applied magnetic field during MRI. The magnetic susceptibility of a device is directly related to its interaction with the MRI system in terms of magnetically induced displacement force, magnetically induced torque, and MR image artifacts [52,67,68]. Both magnetically induced force and torque may trigger unwanted dislodgement or movement of the implant, possibly causing tissue damage or presenting a projectile hazard in a worst-case scenario [37]. The radiofrequency coil of the MRI system can cause heating of the implant or of the adjacent tissue, especially during long scan durations [37]. Therefore, knee implants should ideally be evaluated regarding potential device hazards in a clinically relevant MR test environment before clinical use. This information should be given to both the clinicians and the patients. To the best of our knowledge, all commercially available knee implants in the United States to date are labeled as "MR Conditional" (the device poses no known hazards in a specified MR environment where additional conditions for safe use are met). Moreover, the labels "MR Unsafe" (the device poses known hazards in all MR environments) and "safety in MRI not evaluated" exist, the latter able to be used in certain
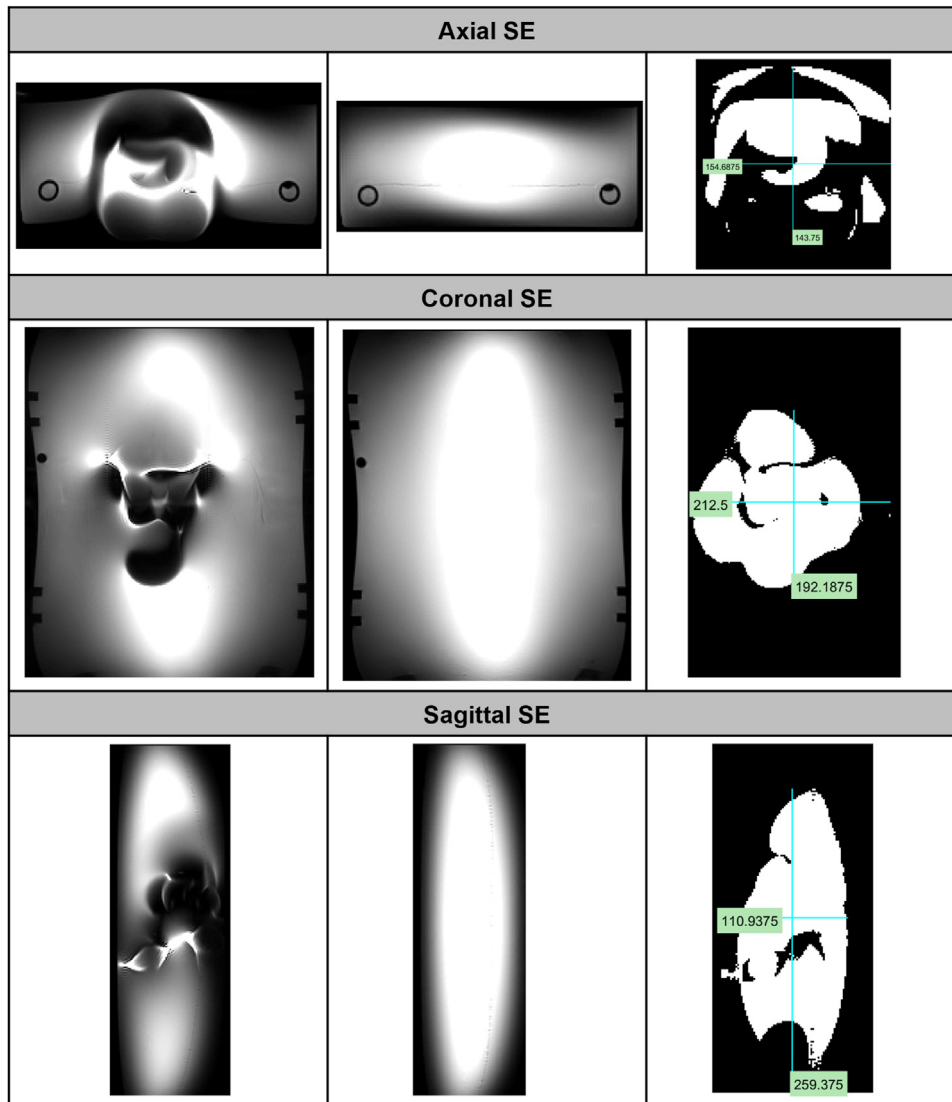
Figure 4. CoCr knee with a spin echo pulse sequence in a 3T MRI system. Worst-case image (left), background image (middle), resulting image artifact (right). Measurements are in millimeters.

circumstances, such as for devices that have historically not provided any MRI safety information [60]. In contrast, and according to ASTM F2503-20 Standard, an item that poses no known hazards resulting from exposure to any MR environment can be marked as "MR Safe." Specifically, MR Safe devices are composed of materials that are electrically nonconductive, nonmetallic, and nonmagnetic [36].

The presented results show that the herein investigated AMC ceramic knee does not pose a significant risk in a clinical MR environment with a static magnetic field of 3T. Moreover, RF-induced heating testing establishes that a patient with the AMC ceramic knee may be safely scanned in a 1.5T or 3T MRI system for 60 minutes in first level operating mode. This was assessed under worst-case scenarios in a heat-insulating gel phantom closest to the radiofrequency coil. These results suggest that the AMC ceramic knee can be labeled as MR safe, meaning that patients with the implant have no scanning restrictions.

Given the broad use of CoCr knee systems in TKA, the maximum image artifact distances between the AMC ceramic knee and a CoCr knee were assessed in a 3T MRI system. Results show that the AMC ceramic knee enables scanning at 3T in and around the implant with minimal image artifacts in comparison to substantially stronger by the CoCr knee. Of note, the best artifact reduction for many metallic devices is obtained using a lower field strength, which is 1.5T in the clinical setting [46], and lower field strengths enable better visualization of the peri-implant region compared to metal artifact reduction techniques used at 3T [52]. This was confirmed for a zirconia femoral implant, producing minimal artifacts both at 1.5 and 3T, compared to significant image artifacts of a CoCr femoral implant, with hardly recognizable shape at 3T [69]. Although 1.5T scanners remain the standard technology in most hospitals to date, 3T scanners come with higher image resolution and a considerably reduced scan time, which is of great value for the patient both in terms of comfort and reduced risk of heating. Thus, the demonstrated safety of the herein tested AMC ceramic knee in 3T scanners provides a significant advantage over other metallic knee implants.

Magnetic susceptibility of the AMC ceramic material (BIOLOX *delta*) was assessed. For comparison, the magnetic susceptibility of medical-grade CoCr and Ti alloys was determined to be 410-1443
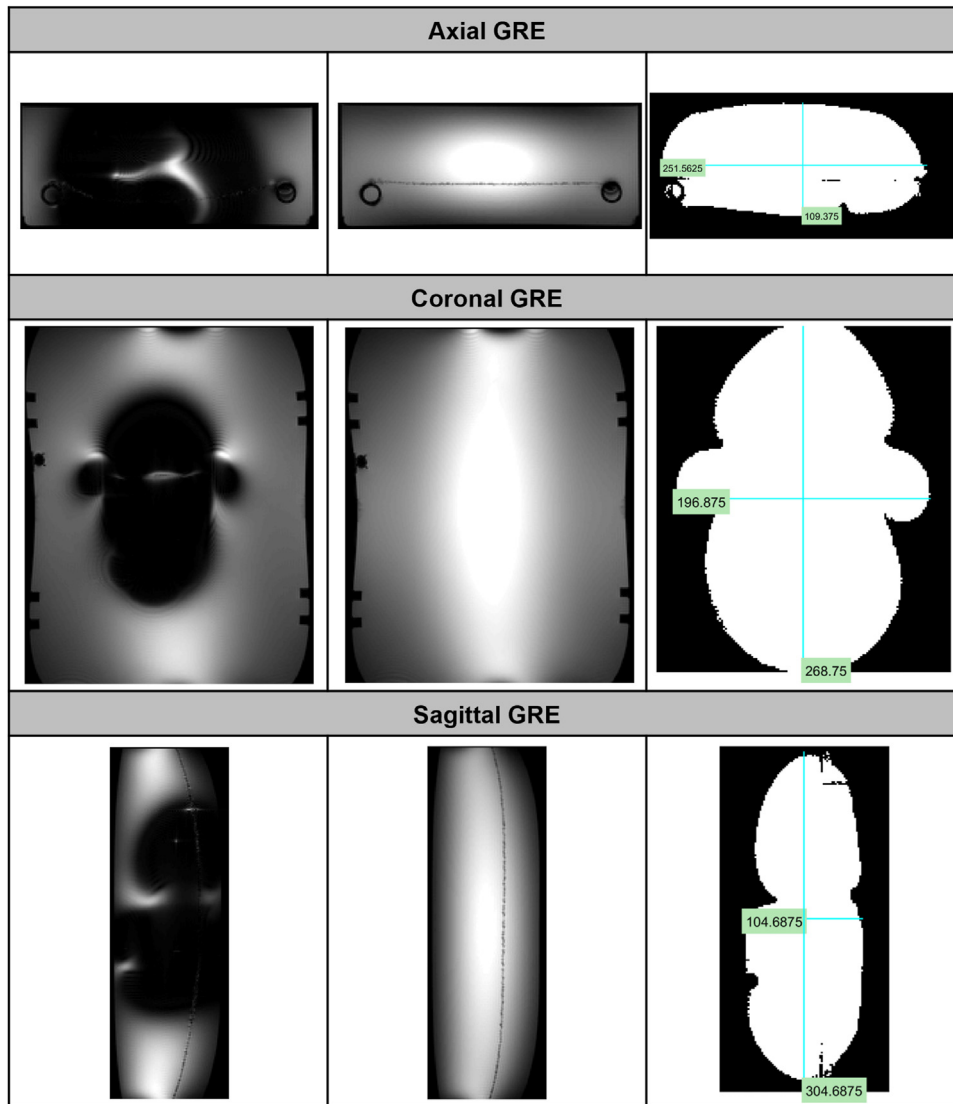
Figure 5. CoCr knee with a gradient echo pulse sequence in a 3T MRI system. Worst-case image (left), background image (middle), resulting image artifact (right). Measurements are in millimeters.

times and 79-95 times higher compared to the AMC ceramic. The magnetic susceptibility of the implant material positively correlated with MR image artifact distance of the scanned knee implant. This correlation between magnetic susceptibility and imaging artifacts was shown for different metal materials before [70].

This in vitro investigation has its limitations, such as not being able to simulate the impact of the implant's surrounding tissues on MR imaging results in vivo. Furthermore, albeit the radiofrequency-induced heating measurements were performed in worst-case scenario in a gel phantom that prevents convection, heating of

Table 3
Summary of the performed hazard tests and image artifact assessment with corresponding pass/fail criterions.

Hazard addressed	Test method	Acceptance criterion	Medical device configuration tested	Summary of test results and pass/fail if appropriate
MR image artifact	ASTM F2119-07(2013) [52]	Information is useful for MR technologist to determine imaging feasibility in the presence of an implant	AMC ceramic knee CoCr knee	Maximum artifact extended 7 mm from AMC ceramic knee and 88 mm from CoCr knee (GRE scan at 3T)
Magnetically induced displacement force	ASTM F2052-21 [49]	Magnetic force less than or equal to device weight (ie, deflection angle $\leq 45°$)	AMC ceramic knee	$0°$ deflection angle at location of maximum force product; pass
Magnetically induced torque	ASTM F2213-17 [50]	Magnetic torque less than gravitational torque	AMC ceramic knee	No observable torque at 3T; pass
RF-induced heating	ASTM F2182-19e2 [51]	CEM43 <16 min No cooling period for 1 h of scanning if temperature rise is less than 4°C after 15 min	AMC ceramic knee	Circularly polarized (CP) body coil, maximum whole-body averaged SAR of 4.0 W/kg. Temperature rise of 2.1°C over 15 min with a CEM43 value of 0 min; pass

Table 4
Volumetric magnetic susceptibility of the materials tested.

Material	Magnetic susceptibility (ppm)
CoCr alloys[a]	820-2885
Ti alloy[b]	157-190
AMC ceramic (BIOLOX *delta*)	2

[a] Measurement range of 2 different alloys and 2 metal working techniques.
[b] Measurement range of 2 metal working techniques.

the device in vivo would likely be different from the obtained values in this experimental setting. The ASTM gel phantom also does not account for the effects of perfusion, which would also lower systemic heating in vivo. Additionally, image artifacts of the implants were assessed in a homogeneous copper sulfate phantom. The actual size and appearance of the artifacts would likely be different in vivo due to the heterogeneous tissue structure. Lastly, this study was not performed with a regulatory approved device, but with a device still under development.

Despite the so far limited use of ceramic components in TKA, their overall safety for in vivo use was recently confirmed, showing rare implant breakage and aseptic loosening [71]. Clinical long-term follow-up data for alumina knee implants are described as good or excellent in patients with rheumatoid arthritis and osteoarthritis [72,73]. AMC ceramic as bicondylar knee component matching with a titanium tibial tray was first in-patient implanted in 2006, and follow-up data showed significantly improved clinical scores and an overall Kaplan-Meier survivorship of 96% at 5 years [74,75]. First clinical data on a metal-free ceramic (BIOLOX *delta*) TKA demonstrated significantly improved clinical scores, no periprosthetic fractures or other sort of implant failure, and comparable performance to a CoCr knee after 1-year follow-up in patients with metal hypersensitivity [76,77]. These observations were confirmed after 4 years in the same patient cohort, ascribing excellent immuno-allergological compatibility to the implant [78]. Recently, this TKA device was tested in vitro in a 1.5T MRI setting, showing a temperature rise of less than $1°C$ and no observed movement or displacement of the device [79].

Clinical trials to prove a positive outcome regarding implant survivorship and clinical effectivity of this novel device are to be performed in the future.

Conclusions

The herein investigated AMC ceramic knee, which is currently under development, is a novel metal-free TKA device that could provide a reasonable and advantageous alternative to commercially available metal knee implants. The AMC ceramic knee is composed of electrically nonconductive, nonmetallic, and nonmagnetic materials. There are no known hazards resulting from exposure of this implant to a magnetic resonance environment, suggesting that the AMC ceramic knee can be regarded as MR Safe. Minimal MR image artifacts at 3T result in high-quality images of the device, qualifying this ceramic TKA device as a valuable alternative to alternative knee implants on the market.

Conflicts of interest

Y. Mödinger and A.A. Porporati are paid employees of CeramTec GmbH. Each author declares that he or she has no commercial associations that might pose a conflict of interest in connection with the submitted article.

For full disclosure statements refer to https://doi.org/10.1016/j.artd.2023.101170.

References

[1] Asif MI. Characterisation and biological impact of wear particles from composite ceramic hip replacements. School of Mechanical Engineering, The University of Leeds; 2018. PhD Thesis.
[2] Cunningham BW, Hallab NJ, Hu N, McAfee PC. Epidural application of spinal instrumentation particulate wear debris: a comprehensive evaluation of neurotoxicity using an in vivo animal model. J Neurosurg Spine 2013;19:336−50.
[3] Zietz C, Bergschmidt P, Lange R, Mittelmeier W, Bader R. Third-body abrasive wear of tibial polyethylene inserts combined with metallic and ceramic femoral components in a knee simulator study. Int J Artif Organs 2013;36:47−55.
[4] Maccauro G, Cittadini A, Magnani G, et al. In vivo characterization of zirconia toughened alumina material: a comparative animal study. Int J Immunopathol Pharmacol 2010;23:841−6.
[5] Maccauro G, Bianchino G, Sangiorgi S, Magnani G, Marotta D, Manicone PF, et al. Development of a new zirconia-toughened alumina: promising mechanical roperties and absence of in vitro carcinogenicity. Int J Immunopathol Pharmacol 2009;22:773−9.
[6] Higuchi Y, Seki T, Morita D, Komatsu D, Takegami Y, Ishiguro N. Comparison of wear rate between ceramic-on-ceramic, metal on highly cross-linked polyethylene, and metal-on-metal bearings. Rev Bras Ortop (Sao Paulo) 2019;54: 295−302.
[7] De Fine M, Terrando S, Hintner M, Porporati AA, Pignatti G. Pushing ceramic-on-ceramic in the most extreme wear conditions: a hip simulator study. J Orthop Traumatol Surg Res 2021;107:102643.
[8] Solarino G, Piconi C, De Santis V, Piazzolla A, Moretti B. Ceramic total knee arthroplasty: ready to go? Joints 2017;05:224−8.
[9] Comitini S, Tigani D, Leonetti D, et al. Evolution in knee replacement implant. Single Cell Biol 2015;04:1−7.
[10] Reiner T, Sorbi R, Müller M, et al. Blood metal ion release after primary total knee arthroplasty: a prospective study. Orthop Surg 2020;12:396−403.
[11] Lützner J, Günther KP, Postler A, Morlock M. Metal ion release after hip and knee arthroplasty - causes, biological effects and diagnostics. Z Orthop Unfall 2020;158:369−82.
[12] Lons A, Putman S, Pasquier G, Migaud H, Drumez E, Girard J. Metallic ion release after knee prosthesis implantation: a prospective study. Int Orthop 2017;41:2503−9.
[13] Mochida Y, Bauer TW, Koshino T, Hirakawa K, Saito T. Histologic and quantitative wear particle analyses of tissue around cementless ceramic total knee prostheses. J Arthroplasty 2002;17:121−8.
[14] Minoda Y, Kobayashi A, Iwaki H, et al. Polyethylene wear particle generation in vivo in an alumina medial pivot total knee prosthesis. Biomaterials 2005;26: 6034−40.
[15] Oonishi H, Ueno M, Kim SC, Oonishi H, Iwamoto M, Kyomoto M. Ceramic versus cobalt-chrome femoral components; wear of polyethylene insert in total knee prosthesis. J Arthroplasty 2009;24:374−82.
[16] Kim KT, Lee S, Ko DO, Seo BS, Jung WS, Chang BK. Causes of failure after total knee arthroplasty in osteoarthritis patients 55 years of age or younger. Knee Surg Relat Res 2014;26:13−9.
[17] Minoda Y, Hata K, Ikebuchi M, Mizokawa S, Ohta Y, Nakamura H. Comparison of in vivo polyethylene wear particles between mobile- and fixed-bearing TKA in the same patients. Knee Surg Sports Traumatol Arthrosc 2017;25:2887−93.
[18] Drummond J, Tran P, Fary C. Metal-on-metal hip arthroplasty: a review of adverse reactions and patient management. J Funct Biomater 2015;6:486−99.
[19] Hosman AH, van der Mei HC, Bulstra SK, Busscher HJ, Neut D. Effects of metal-on-metal wear on the host immune system and infection in hip arthroplasty. Acta Orthop 2010;81:526−34.
[20] Chisari E, Magnuson J, Ong C, Parvizi J, Krueger CA. Ceramic-on-polyethylene hip arthroplasty reduces the risk of post-operative periprosthetic joint infection. J Orthop Res 2022;40:2133−8.
[21] Lenguerrand E, Whitehouse MR, et al. Risk factors associated with revision for prosthetic joint infection after hip replacement: a prospective observational cohort study. Lancet Infect Dis 2018;18:1004−14.
[22] Pitto RP, Sedel L. Periprosthetic joint infection in hip arthroplasty: is there an association between infection and bearing surface type? Clin Orthop Relat Res 2016;474:2213−8.
[23] Madanat R, Laaksonen I, Graves SE, et al. Ceramic bearings for total hip arthroplasty are associated with a reduced risk of revision for infection. Hip Int 2018;28:222−6.
[24] Renner L, Perka C, Melsheimer O, Grimberg A, Volkmar J, Steinbruck A. Ceramic-on-ceramic bearing in total hip arthroplasty reduces the risk for revision for periprosthetic joint infection compared to ceramic-on-polyethylene: a matched analysis of 118,753 cementless THA based on the German Arthroplasty Registry. J Clin Med 2021;10:1193.
[25] Holleyman RJ, Critchley RJ, Mason JM, Jameson SS, Reed MR, Malviya A. Ceramic bearings are associated with a significantly reduced revision rate in primary hip arthroplasty: an analysis from the National Joint Registry for England, Wales, Northern Ireland, and the Isle of Man. J Arthroplasty 2021;36: 3498−506.
[26] van der Merwe JM. Metal hypersensitivity in joint arthroplasty. J Am Acad Orthop Surg Glob Res Rev 2021;5:e20.00200.
[27] Podzimek S, Himmlova L, Janatova T, et al. Metal hypersensitivity and proinflammatory cytokine production in patients with failed orthopedic implants: a case-control study. Clin Immunol 2022;245:109152.

[28] Schalock PC, Menné T, Johansen JD, et al. Hypersensitivity reactions to metallic implants - diagnostic algorithm and suggested patch test series for clinical use. Contact Dermatitis 2012;66:4–19.

[29] Thomas P, Summer B. Diagnosis and management of patients with allergy to metal implants. Expert Rev Clin Immunol 2015;11:501–9.

[30] Richards LJ, Streifel A, Rodrigues JM. Utility of patch testing and lymphocyte transformation testing in the evaluation of metal allergy in patients with orthopedic implants. Cureus 2019;11:e5761.

[31] Bracey DN, Hegde V, Johnson R, et al. Poor correlation among metal hypersensitivity testing modalities and inferior patient-reported outcomes after primary and revision total knee arthroplasties. Arthroplasty Today 2022;18:138–42.

[32] Yang S, Dipane M, Lu CH, Schmalzried TP, McPherson EJ. Lymphocyte transformation testing (LTT) in cases of pain following total knee arthroplasty: little relationship to histopathologic findings and revision outcomes. J Bone Joint Surg Am 2019;101:257–64.

[33] Christensen JC, Kittelson AJ, Loyd BJ, Himawan MA, Thigpen CA, Stevens-Lapsley JE. Characteristics of young and lower functioning patients following total knee arthroplasty: a retrospective study. BMC Musculoskelet Disord 2019;20:483.

[34] George LK, Hu L, Sloan FA. The effects of total knee arthroplasty on physical functioning and health among the under age 65 population. Value Health 2014;17:605–10.

[35] Keeney JA, Eunice S, Pashos G, Wright RW, Clohisy JC. What is the evidence for total knee arthroplasty in young patients?: a systematic review of the literature. Clin Orthop Relat Res 2011;469:574–83.

[36] Walker-Santiago R, Tegethoff JD, Ralston WM, Keeney JA. Revision total knee arthroplasty in young patients: higher early reoperation and rerevision. J Arthroplasty 2021;36:653–6.

[37] Mosher ZA, Sawyer JR, Kelly DM. MRI safety with orthopedic implants. Orthop Clin North Am 2018;49:455–63.

[38] Orthopedic Network News. 2022 hip and knee implant review. Orthopedic Netw News 2022;33:1–23.

[39] Singh JA, Yu S, Chen L, Cleveland JD. Rates of total joint replacement in the United States: future projections to 2020-2040 using the National Inpatient Sample. J Rheumatol 2019;46:1134–40.

[40] Sneag DB, Bogner EA, Potter HG. Magnetic resonance imaging evaluation of the painful total knee arthroplasty. Semin Musculoskelet Radiol 2015;19:40–8.

[41] Schröder FF, Post CE, Wagenaar FBM, Verdonschot N, Huis In't Veld RMHA. MRI as diagnostic modality for analyzing the problematic knee arthroplasty: a systematic review. J Magn Reson Imaging 2020;51:446–58.

[42] Galley J, Sutter R, Stern C, Filli L, Rahm S, Pfirrmann CWA. Diagnosis of periprosthetic hip joint infection using MRI with metal artifact reduction at 1.5 T. Radiology 2020;296:98–108.

[43] Potter HG, Nestor BJ, Sofka CM, Ho ST, Peters LE, Salvati E. Magnetic resonance imaging after total hip arthroplasty: evaluation of periprosthetic soft tissue. J Bone Joint Surg Am 2004;86:1947–54.

[44] Padgett DE, Su EP, Wright TM, Burge AJ, Potter HG. How useful is magnetic resonance imaging in evaluating adverse local tissue reaction? J Arthroplasty 2020;35:S63–7.

[45] Chang EY, Bae WC, Chung CB. Imaging the knee in the setting of metal hardware. Magn Reson Imaging Clin N Am 2014;22:765–86.

[46] Koff MF, Burge AJ, Potter HG. Clinical magnetic resonance imaging of arthroplasty at 1.5 T. J Orthop Res 2020;38:1455–64.

[47] Xiong L, Smith EJ, Klemt C, Barghi A, Padmanabha A, Kwon YM. MRI characteristics of adverse local tissue reactions associated with intraoperative tissue damage and poor revision surgery outcomes: a systematic review. J Am Acad Orthop Surg 2021;29:e1025–33.

[48] Fritz J, Lurie B, Potter HG. MR imaging of knee arthroplasty implants. Radiographics 2015;35:1483–501.

[49] Koff MF, Shah P, Potter HG. Clinical implementation of MRI of joint arthroplasty. AJR Am J Roentgenol 2014;203:154–61.

[50] Khodarahmi I, Isaac A, Fishman E, Dalili D, Fritz J. Metal about the hip and artifact reduction techniques: from basic concepts to advanced imaging. Semin Musculoskelet Radiol 2019;23:e68–81.

[51] Koch KM, Hargreaves BA, Pauly KB, Chen W, Gold GE, King KF. Magnetic resonance imaging near metal implants. J Magn Reson Imaging 2010;32:773–87.

[52] Germann C, Nanz D, Sutter R. Magnetic resonance imaging around metal at 1.5 Tesla: techniques from basic to advanced and clinical impact. Invest Radiol 2021;56:734–48.

[53] Khodarahmi I, Fishman EK, Fritz J. Dedicated CT and MRI techniques for the evaluation of the postoperative knee. Semin Musculoskelet Radiol 2018;22:444–56.

[54] Jahwar A, Reichert M, Kostrzewa M, et al. Usefulness of slice encoding for metal artifact correction (SEMAC) technique for reducing metal artifacts after total knee arthroplasty. Eur J Orthop Surg Traumatol 2019;29:659–66.

[55] Fehring TK, Fehring K, Odum SM. Metal artifact reduction sequence MRI abnormalities occur in metal-on-polyethylene hips. Clin Orthop Relat Res 2015;473:574–80.

[56] ASTM F2052-21. Standard test method for measurement of magnetically induced displacement force on medical devices in the magnetic resonance environment. West Conshohocken, PA: ASTM International; 2021.

[57] ASTM F2213-17, Standard test method for measurement of magnetically induced torque on medical devices in the magnetic resonance environment. West Conshohocken, PA: ASTM International; 2017.

[58] ASTM F2182-19e2, Standard test method for measurement of radio frequency induced heating on or near passive implants during magnetic resonance imaging. West Conshohocken, PA: ASTM International; 2019.

[59] ASTM F2119-07, Standard test method for evaluation of MR image artifacts from passive implants. West Conshohocken, PA: ASTM International; 2013.

[60] FDA. Guidance Document_Testing and labeling medical devices for safety in the magnetic resonance (MR) environment. FDA Health; 2021.

[61] ASTM F2503-20, Standard practice for marking medical devices and other items for safety in the magnetic resonance environment. West Conshohocken, PA: ASTM International; 2020.

[62] Kurtz SM, Lau E, Ong K, Zhao K, Kelly M, Bozic KJ. Future young patient demand for primary and revision joint replacement: national projections from 2010 to 2030. Clin Orthop Relat Res 2009;467:2606–12.

[63] Leppänen S, Niemelainen M, Huhtala H, Eskelinen A. Mild knee osteoarthritis predicts dissatisfaction after total knee arthroplasty: a prospective study of 186 patients aged 65 years or less with 2-year follow-up. BMC Musculoskelet Disord 2021;22:657.

[64] Dunbar MJ, Richardson G, Robertsson O. I can't get no satisfaction after my total knee replacement. Bone Joint J 2013;95-B(11_Supple_A):148–52.

[65] Bourne RB, Chesworth BM, Davis AM, Mahomed NN, Charron KD. Patient satisfaction after total knee arthroplasty: who is satisfied and who is not? Clin Orthop Relat Res 2010;468:57–63.

[66] Nakano N, Shoman H, Olavarria F, Matsumoto T, Kuroda R, Khanduja V. Why are patients dissatisfied following a total knee replacement? A systematic review. Int Orthop 2020;44:1971–2007.

[67] Kajima Y, Takaichi A, Tsutsumi Y, Hanawa T, Wakabayashi N, Kawasaki A. Influence of magnetic susceptibility and volume on MRI artifacts produced by low magnetic susceptibility Zr-14Nb alloy and dental alloys. Dent Mater J 2020;39:256–61.

[68] Schenck JF. The role iof magnetic susceptibility in MRI. Magnetic compatibility of the first and second kinds. Med Phys 1996;23:815–50.

[69] Kamishima T, Kitamura N, Amemiya M, et al. Experimental MR imaging of zirconia ceramic joint implants at 1.5 and 3 T. Clin Radiol 2010;65:387–90.

[70] Baker GM, Anttila E, Smith E, Robison A, Gross DC. Magnetic susceptibility of common metals and alloys used in medical devices. London: ISMRM - The International Society for Magnetic Resonance in Medicine; 2022.

[71] Xiang S, Zhao Y, Li Z, Feng B, Weng X. Clinical outcomes of ceramic femoral prosthesis in total knee arthroplasty: a systematic review. J Orthop Surg Res 2019;14:57.

[72] Nakamura S, Ito H, Nakamura K, Kuriyama S, Furu M, Matsuda S. Long-term durability of ceramic tri-condylar knee implants: a minimum 15-year follow-up. J Arthroplasty 2017;32:1874–9.

[73] Koshino T, Okamoto R, Takagi T, Yamamoto K, Saito T. Cemented ceramic YMCK total knee arthroplasty in patients with severe rheumatoid arthritis. J Arthroplasty 2002;17:1009–15.

[74] Bergschmidt P, Bader R, Ganzer D, et al. Prospective multi-centre study on a composite ceramic femoral component in total knee arthroplasty: five-year clinical and radiological outcomes. Knee 2015;22:186–91.

[75] Bergschmidt P, Kluess D, Zietz C, Finze S, Bader R, Mittelmeier W. Composite ceramics in total knee arthroplasty: two-year experience in clinical application. Semin Arthroplasty 2011;22:264–70.

[76] Meier E, Gelse K, Trieb K, Pachowsky M, Hennig FF, Mauerer A. First clinical study of a novel complete metal-free ceramic total knee replacement system. J Orthop Surg Res 2016;11:21.

[77] Trieb K, Ullmann D, Metzinger K, et al. Prospective comparison of a metal-free ceramic total knee arthroplasty with an identical metal system. Z Orthop Unfall 2018;156:46–52.

[78] Breuer R, Fiala R, Trieb K, Rath B. Prospective mid-term results of a completely metal-free ceramic total knee endoprothesis: a concise follow-up of a previous report. J Arthroplasty 2021;36:3161–7.

[79] Trieb K, Artmann A, Krupa M, Senck S, Landauer F. Evaluation of temperature of a full ceramic total knee arthroplasty during MRI examinations. Medicine (Baltimore) 2022;101:e30685.

Equations

Magnetically induced torque was calculated according to according to Equation S1:

$$\tau_{mag} \leq \mu_s mgl \qquad \text{Equation S1}$$

where τ_{mag} is the magnetically induced torque, μ_s is the coefficient of static friction, m is the mass of the implant, g is the acceleration due to gravity, and l is the length of the implant.

The measured temperature rise was calculated using Equation S2. Temperature rise scaled to a whole phantom average specific absorption rate (SAR) was calculated using Equation S3.

$$\Delta T_i(t) = T_i(t) - T_i(0) \qquad \text{Equation S2}$$

$$\Delta T_{i,4.0}(t) = \Delta T_i(t) \cdot \phi \qquad \text{Equation S3}$$

where $\Delta T_i(t)$ is the measured temperature rise of the i-th probe at time t, $\Delta T_{i,4.0}(t)$ is the temperature rise of the i-th probe at time t scaled to a whole phantom average SAR of 4.0 W/kg, $T_i(t)$ is the temperature of i-th probe at time t, ϕ is the SAR scale factor $= 4.0$ W/kg/$SAR_{measured}$, and $SAR_{measured}$ is the whole phantom average SAR measured with a calibration rod test and simulation (W/kg).

Table S1
MRI scanning acquisition mode for evaluation of RF-induced heating on a 3T MRI system (Discovery MR750 [GE Healthcare]).

Parameters	Values
Pulse sequence	FSE
Repetition time (TR)	400 ms
Echo time (TE)	14 ms
Flip angle	125°
Pixel bandwidth	19 Hz/px
Acquisition matrix	256 × 256
Slice thickness	10 mm
Total slices	42
Scan time duration	15 min
GE: transmit gain	135 counts
B1+RMS, scanner reported	2.13 μT
Real-time power deposition monitor, 10 s average	1.3 W/kg

Table S2
MRI scanning acquisition mode for image artifact testing on a 3T MRI system (MAGNETOM Prisma [Siemens Healthcare GmbH]).

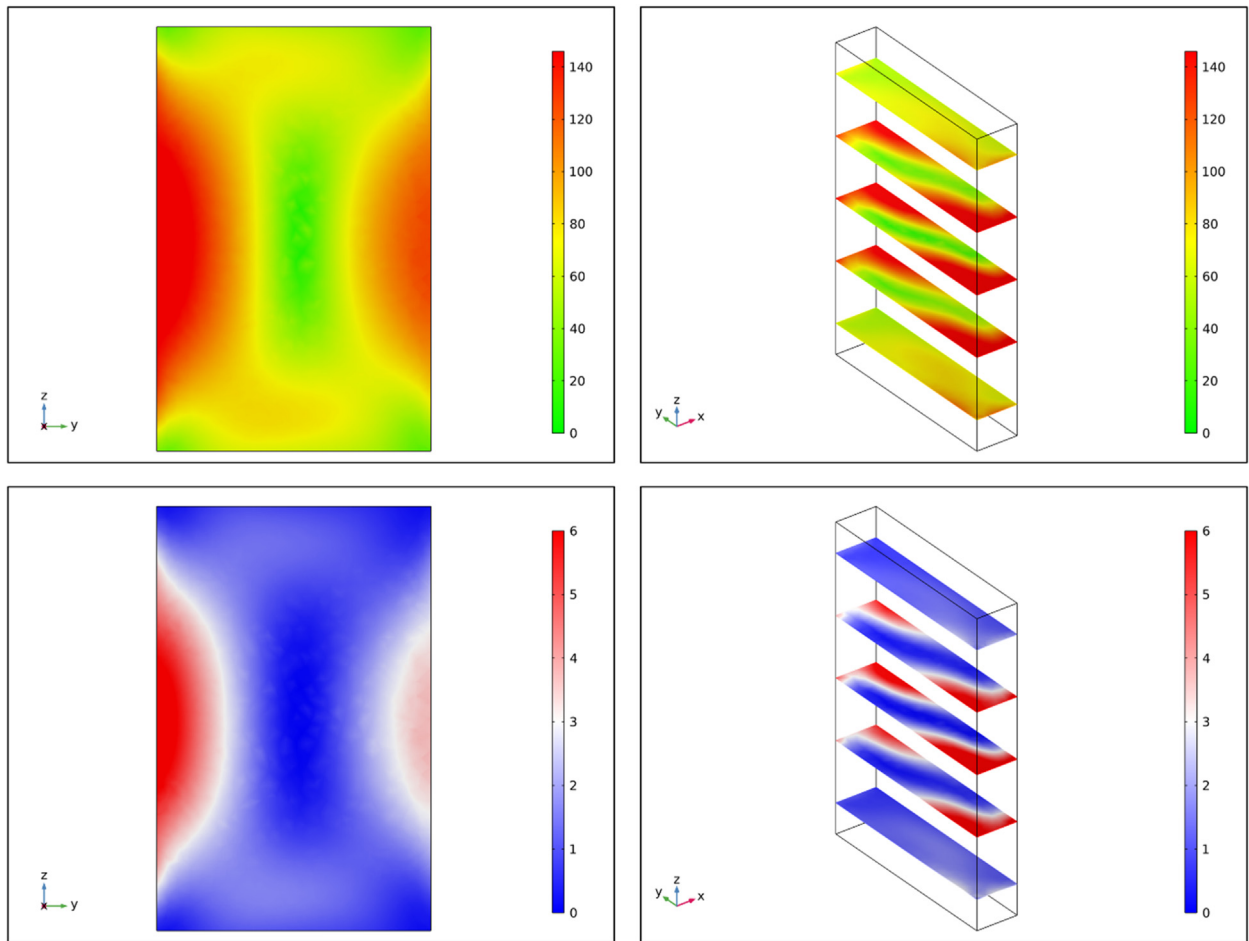| Parameters	Pulse sequence 1	Pulse sequence 2
Type of pulse sequence	Gradient spin echo	Spin echo
Repetition time (TR)	100 ms	500 ms
Echo time (TE)	10 ms	20 ms
Flip angle	30°	50°
Pixel bandwidth	120 Hz/px	125 Hz/px
Acquisition matrix	256 × 256	256 × 256
Slice thickness	10 mm	10 mm
Transmit coil	Body	Body
Receiver coil	Body	Body

Fig. S1. Slices through the empty gel phantom of electric field in V/m (top) and SAR in W/kg (bottom) for simulated RF application in a 3T/123 MHz MRI system. Computational analysis of the gelled saline phantom showed that the left side of the gelled saline phantom is associated with a greater electrical field. Thus, the test article was positioned on the far-left side of the gelled saline phantom (not shown).
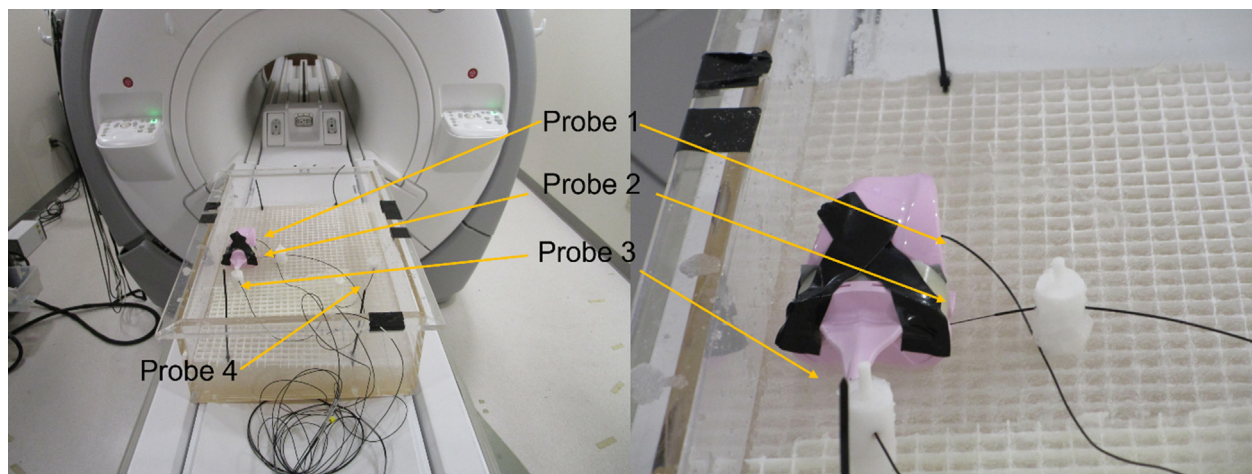

Fig. S2. Fiber Optic Thermometry Probe locations during RF-induced heating evaluation on a 3T MRI system (Discovery MR750 [GE Healthcare]). Three probes were placed on the implant. The fourth probe served as a reference and was located on the opposite side of the gel phantom.